A Continuous Tone Model of Halftones

J.S. Arney,▲ Prashant Mehta and Peter G. Anderson▲

Center for Imaging Science, Rochester Institute of Technology, Rochester, New York, USA

An experimental analysis of Floyd–Steinberg and clustered dot halftones printed with both cyan and black toner on both 300 dpi and 600 dpi laser electrophotographic printers. The printed halftone ramps were measured as reflectance, R, versus coverage of toner, C in units of mass/area. Gravimetric analysis was used to measure coverage. Rather than modeling tone reproduction as a bilevel model of discrete dots on paper, the images were modeled as contiguous layers of colorant on paper. Both the Beer–Lambert and Kubelka–Munk laws were applied. Just as ideal bilevel halftone models require significant modifications to fit experimental data, so too were modifications of the continuous tone model required. The ideal continuous tone model tended to over-compensate for the traditional halftone corrections called "dot-gain". Thus, the corrections applied to the continuous tone model were called ink "anti-gain" to emphasize the analogy with bilevel models. The resulting corrections resulted in reasonably good agreement between the model and the data. Moreover, exploring some of the characteristics of the model indicated a reasonable physical interpretation of the corrections that were applied.

Journal of Imaging Science and Technology 48: 45–49 (2004)

Introduction

A halftone is generally thought of as a bilevel representation of an image, as illustrated in Fig. 1, with ink dots of reflectance R_k and paper with a reflectance of R_g.[1] However, microscopic examination of printed halftones typically shows a bimodal distribution of gray values, and often each distribution consists of a wide range of gray values.[2,3] Nevertheless, bilevel models have been applied successfully for decades to describe tone reproduction in printed halftone images. The success of these bilevel models has been achieved largely by making significant modifications to account for the wide distribution of gray values in the actual image. In the current work, we describe an alternative approach for modeling printed halftone images that does not assume a bilevel, or even a bimodal image. The model is constructed by assuming that the printed image is actually a continuous tone image, composed of a contiguous image layer on paper, and modifications are applied to correct for spatial effects.

The Bilevel Approximation

Analysis of tone reproduction for halftones generally begins with a bilevel model based on the Murray–Davies equation, (Eq. (1)). The term F_n is the dot area fraction the printing engine is told to print. The dot area fraction is the heart of the bilevel assumption.

$$R = F_n \cdot R_k + (1 - F_n) \cdot R_g \tag{1}$$

When a halftone is actually printed, problems with Eq. (1) emerge. In particular, if R_k and R_g are the reflectance values of the image at $F_n = 0$ (solid ink) and $F_n = 1$ (blank paper), the printed image at any $0 < F_n < 1$ is almost always darker than predicted by Eq. (1). When this darkening effect was first noted, it was termed "dot gain".[4,5] The assumption behind this term is that the printed halftone image must be a bilevel image. Then the only way the measured reflectance, R_m, can be darker than the predicted reflectance, R, is for the printed dot size, F, to be larger then the dot size, F_n, sent to the printer. It follows from this reasoning that one should be able to measure the printed reflectance and calculate the printed dot size by a rearrangement of the Murray–Davies equation, as shown in Eq. (2). Then dot gain can be defined quantitatively as in Eq. (3).[4,5]

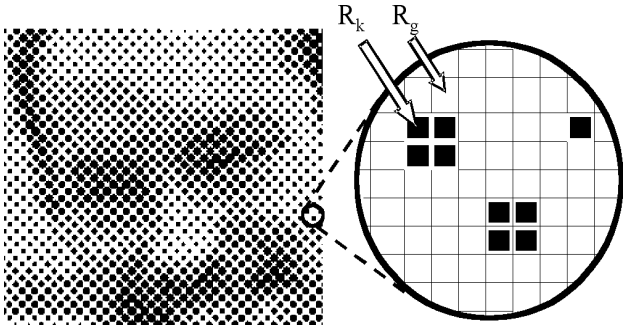

Figure 1. Illustration of a bilevel representation of an image.

$$F = \frac{R_g - R_m}{R_g - R_k} \tag{2}$$

$$\text{Dot Gain} = (F - F_n) \tag{3}$$

Equations (2) and (3) maintain the bilevel approximation of a halftone image, but closer analysis reveals the printed image is not bilevel at all. Figure 2 shows a sample of a clustered dot halftone printed with an offset lithographic printer at 150 lpi. The reflectance histogram is clearly not

Original manuscript received March 12, 2003

▲ IS&T Member

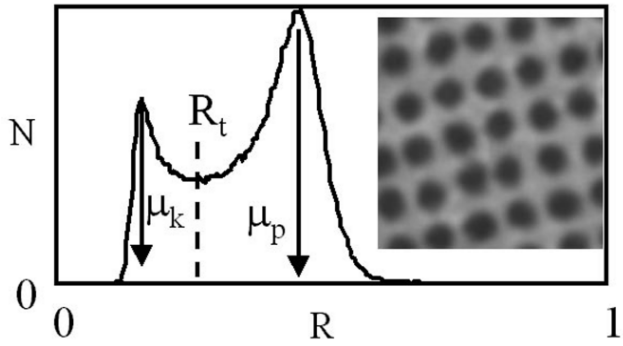

Figure 2. Reflectance histogram of a cyan ink printed as a 150 lpi clustered dot halftone printed on an offset lithographic printer.

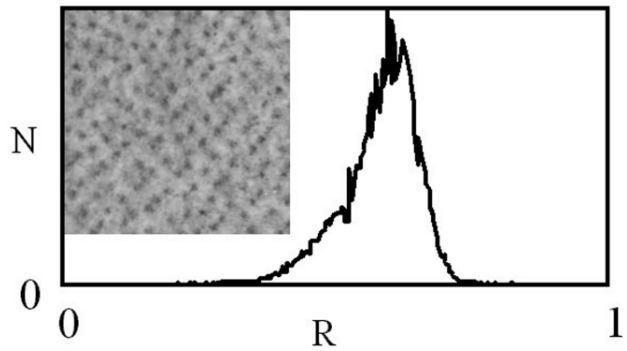

Figure 3. Reflectance histogram for a black toner printed on paper with a Floyd–Steinberg pattern using a 600 dpi electrophotographic printer.

the histogram of a bilevel image. However, it is a bimodal distribution, so we can still maintain the bilevel approximation by defining a dot fraction, F_m, based on some threshold value R_t and two mean gray levels, μ_k and μ_p. Experimentally it is observed that μ_k and μ_p are not constants, but vary with F_n.[2,3] Nevertheless, with careful experimental definitions of F_m, μ_k and μ_p one can maintain the bilevel approximation and model tone reproduction with a form of Murray–Davies shown as Eq. (4).[2,3]

$$R = F_m \cdot \mu_k + (1 - F_m) \cdot \mu_p \tag{4}$$

If one prints a higher frequency halftone image, the bilevel approximation becomes more difficult to describe. Figure 3 shows an example for a Floyd–Steinberg halftone printed with a 600 dpi electrophotographic laser-jet printer. In this system, a change in the gray level command sent to the printer, F_n, results in a shift in the mean value of the histogram rather than a change in the proportion of two peaks. In other words, the image behaves more like a continuous tone image than a halftone, and it becomes more difficult and arbitrary to define metrics F_m, μ_k and μ_p for a bimodal model. Nevertheless, the bilevel approximation is still used extensively to model high frequency halftones.

The Continuous Tone Approximation

Corrections needed to force a bilevel model to fit experimental data focus on the so called "dot gain" effects. These effects seem to increase the probability that an ink dot will absorb light compared to the ideal Murray–Davies case. We have explored an alternative model that starts with the assumption that the halftone image is a continuous tone image. Corrections to force the continuous tone model to fit experimental data also focus on spatial effects of light absorption probability.

To illustrate the development of a modified continuous tone model, we begin with the ideal image illustrated in Fig. 4. This image consists of a contiguous image layer L mm thick. The image layer consists of colorant at a coverage of C in mass/area. The transmission density of the image layer is $D_T = \varepsilon \cdot C$, where ε is the extinction coefficient of the colorant in units mm²/mg and represents the absorption probability of the ink. The reflection density of the paper is $D_g = -\log(R_g)$, so the overall reflection density of the image, $D = -\log(R)$, is given by Eq. (5).

$$D = 2 \cdot \varepsilon \cdot C + D_g \tag{5}$$

Equation (5) can be compared with experimental data for black toner printed with the 600 dpi printer using a

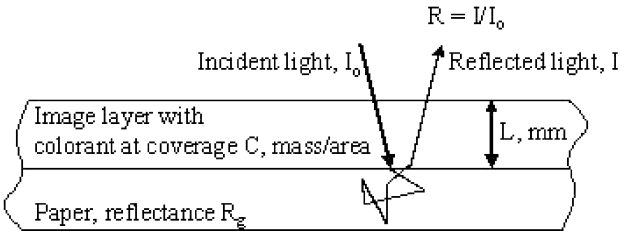

Figure 4. Continuous tone model

Floyd–Steinberg halftone, illustrated in Fig. 3. The model is calibrated with a measurement of the unprinted paper, D_g, and a measurement of the image printed at $F_n = 1$, D_{max}. The coverage is expressed in relative units so C = 1 at D_{max}. The value of ε is then calculated from Eq. (5) as $\varepsilon = 1/2(D - D_g)$ in relative units of mm². From gravimetric analysis of printed samples, it was found that coverage was directly proportional to the print command, F_n, for the 600 dpi printer. Thus, substitution of C for F_n in Eq. (5) results in the solid lines shown in Fig. 5. For comparison, the Murray–Davies model is also shown.

The ideal bilevel model of Murray–Davies is linear in R versus F_n, and the ideal continuous tone model of Beer–Lambert is linear in D versus F_n. In the example shown in Fig. 5, neither model rationalizes the data.

The First Correction: Scattering

The Beer–Lambert model assumes no light scattering in the image layer. However, solid toner can be expected to have a significant scattering coefficient. To account for this scattering, Kubelka–Munk theory was applied as a continuous tone model, as shown in Eq. (6), where S is a scattering coefficient in mm⁻¹, and K is an absorption coefficient in mm⁻¹.[6] The value of K is related to ε, L, and coverage, C, as shown.

$$R = \frac{1 - R_g \cdot \left[a - b \cdot \mathrm{Coth}(b \cdot S \cdot L)\right]}{a - R_g + b \cdot \mathrm{Coth}(b \cdot S \cdot L)} \tag{6}$$

where

$$a = 1 + \frac{K}{S} \qquad b = \sqrt{a^2 - 1} \qquad K = 2.303 \cdot \varepsilon \cdot \frac{C}{L}$$

The continuous tone model based on Kubelka–Munk introduces two parameters, S and L, that were not in the Beer–Lambert model. In addition, the value of ε

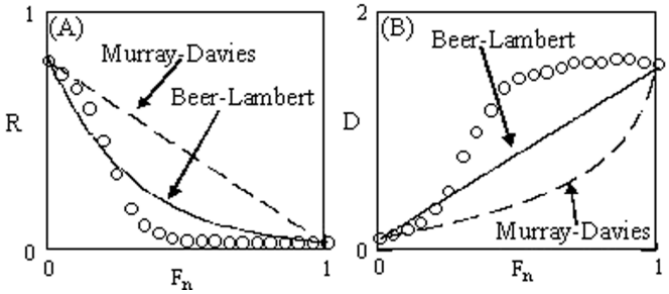

Figure 5. Comparison between the ideal Beer–Lambert model and the ideal Murray–Davies model and experimental data black toner printed with the 600 dpi electrophotographic printer using a Floyd–Steinberg halftone.

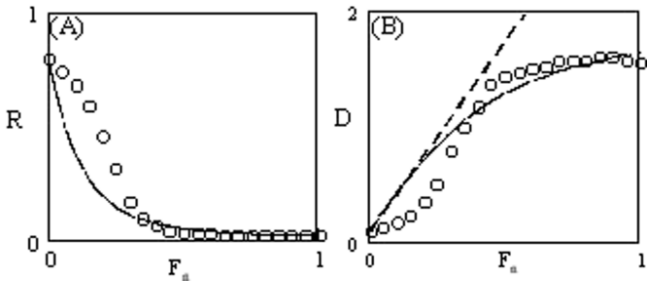

Figure 6. The halftone data from Fig. 4. The solid line is the Kubelka–Munk continuous tone model with $\varepsilon = 5\ mm^2$, $S = 90\ mm^{-1}$, and $L = 0.01$ mm. The dashed line is same model but with $S = 0$.

could no longer be estimated experimentally as $\varepsilon = 1/2(D - D_g)$. Thus the values of ε, S, and L were adjusted arbitrarily to fit the data. Figure 6 shows the result for $\varepsilon = 5\ mm^2$, $S = 90\ mm^{-1}$ and $L = 0.01$ mm.

Figure 6 shows that the Kubelka–Munk model provides a rationale for the effect of scattering on tone reproduction. However, the model still greatly over-estimates the so-called "dot gain" effect and models the mid-tone gray values far darker than they are experimentally. To account for this, the continuous tone model requires a spatial modification we call "ink anti-gain".

The Second Correction: Ink Anti-gain

The concept of ink anti-gain is analogous to dot gain. It is a spatial effect in which the probability of absorption of light decreases as the spatial frequency of the halftone decreases. In other words, the continuous tone model assumes that the ink can be characterized by an extinction coefficient, ε_o. It is assumed the value of ε_o applies to all halftones at $F_n = 1$ and to all values of F_n for an infinitely high frequency halftone. At finite frequencies and $F_n < 1$, the effective value of ε decreases, $\varepsilon < \varepsilon_o$. The concept of a variable ε is essentially a mirror image of the concept of dot gain, so we use the term "ink anti-gain". As the value of F_n decreases, the absorption efficiency of the ink decreases. We modeled the ink anti-gain effect empirically as shown in Eq. (7) with the efficiency function, $f(F_n)$ shown in Eq. (8).

$$\varepsilon(F_n) = f(F_n) \cdot \varepsilon_o \tag{7}$$

$$f(F_n) = \frac{1}{1 + \exp\{-k(F_n - F_c)\}} \tag{8}$$

For an image layer with a significant scattering coefficient, S, it is necessary to model S as a function of coverage. Otherwise, the modeled R will not approach R_g as C approaches 0. The function used in this model is shown in Eq. (9).

$$S(C) = S_o \cdot C \tag{9}$$

Combining Eqs. (6), (7), (8), and (9) forms a continuous tone model with ink anti-gain correction with adjustable constants S_o, L, ε_o, k and F_c. Adjusting these values produces reasonably good agreement with experimental data, as illustrated in Fig. 7.

Figure 7 also compares the model and experimental data for black toner printed with a 300 dpi laserjet using a Floyd–Steinberg pattern. For the 300 dpi printer, gravimetric analysis revealed a non-linear relationship between F_n and C, which was modeled with a 2nd order polynomial.

Halftone ramps were printed with both the 300 and the 600 dpi printers using both a black and a cyan toner, with both a Floyd–Steinberg and a traditional clustered dot pattern. All combinations were printed and modeled with Eqs. (6) through (9). The values of the parameters used to fit the data are shown in Table I.

Exploring the Limits

The agreement between the data and the model, as summarized in Table I, is not too surprising since the model contains five adjustable parameters. Thus, it is of interest to explore the values of the parameters used to fit the data to see if they make physical sense. In particular, changes in toner (black vs cyan), changes in printer (300 vs 600 dpi) and changes in halftone type (Floyd–Steinberg versus Clustered dot) should result in rational changes in the ink absorption efficiency (constants k and F_c) invoked for this model. To explore these effects, we begin by examining characteristics of the absorption efficiency function, f(C).

We begin with the simplest case of $S = 0$ so that Eq. (6) reduces to Eq. (5). Combining this with Eq. (7) and solving for the efficiency function, f(C), we have Eq. (10). Knowing the relationship between C and F_n for both the 600 dpi printer (linear) and the 300 dpi printer (polynomial), we can measure all of the terms in Eq. (10) and calculate experimental values of absorption efficiency, f, for each gray value on the printed ramp. Some results for the 300 dpi printer are shown in Fig. 8. The solid lines were drawn from the model Eq. (8) using the corresponding model parameters in Table I. The results indicate the empirical choice of Eq. (8) is a useful approximation of the process.

$$f(C) = \frac{D(C) - D_g}{2 \cdot \varepsilon_o \cdot C} \tag{10}$$

The area under the curve of f(C) versus C was chosen as a metric for comparing the relative absorption efficiency of each printing system. This metric, calculated from the model equations, is shown as A_{eff} in Table I and has a value in the range $0 \le A_{eff} \le 1$. In addition, a single spatial frequency metric can be defined as the lines per inch (lpi) of the halftone. These are also shown in Table I. Both the printer addressability (dpi) and the halftone pattern determine the overall lpi of the pattern. Figure 9 shows A_{eff} versus lpi for all of the printed samples of Table I. The dashed lines were hand sketched to suggest trends. It is apparent that the

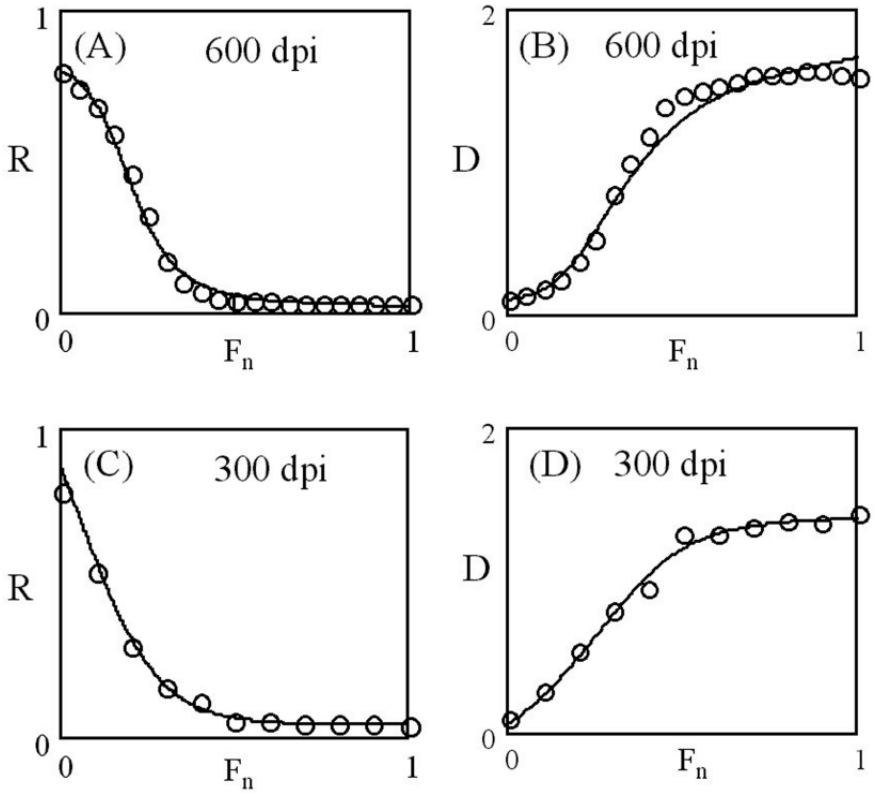

Figure 7. R versus F_n and D versus F_n for 300 and 600 dpi printers using black toner and Floyd–Steinberg. Measured data are indicated with circles, and the Kubelka–Munk model with a variable ε is ——. Fit parameters for both printers are: 600 dpi: ε_o 5 mm^2, S = 90 mm^{-1}, L = 0.01 mm, F_c = 0.40, and k = 9; 300 dpi: ε_o = 4.3 mm^2, S = 90 mm^{-1}, L = 0.01 mm, F_c = 0.50, and k = 6.

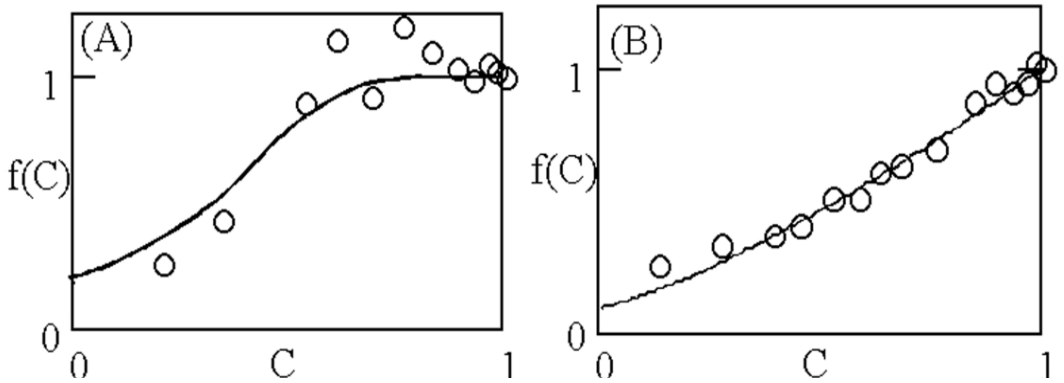

Figure 8. Experimentally estimated efficiency functions, f(C) for the 300 dpi printer using cyan toner and (A) Floyd–Steinberg and (B) a clustered dot halftone. Lines are Eq. (8) with the parameters shown in Table I.

TABLE I. Fit Parameters for the Modified Kubelka–Munk Continuous Tone Model

Printer dpi	Halftone Pattern	Toner	Dot Pitchlines/inch	F_c	k	A_{eff}	$\varepsilon_{o\,mm}{}^2$	S_o mm^{-1}	L mm
600	F–S	Black	600 lpi	0.40	9	0.60	5.0	90	0.01
600	CL	Black	120 lpi	0.50	6	0.50	4.3	90	0.01
600	F–S	Cyan	600 lpi	0.20	9	0.78	0.48	0	—
600	CL	Cyan	120 lpi	0.33	5	0.64	0.36	0	—
300	F–S	Black	300 lpi	0.40	9	0.60	5.0	90	0.23
300	CL	Black	60 lpi	0.80	5	0.26	5.0	90	0.23
300	F–S	Cyan	300 lpi	0.10	15	0.89	0.34	0	—
300	CL	Cyan	60 lpi	0.23	5	0.72	0.34	0	—

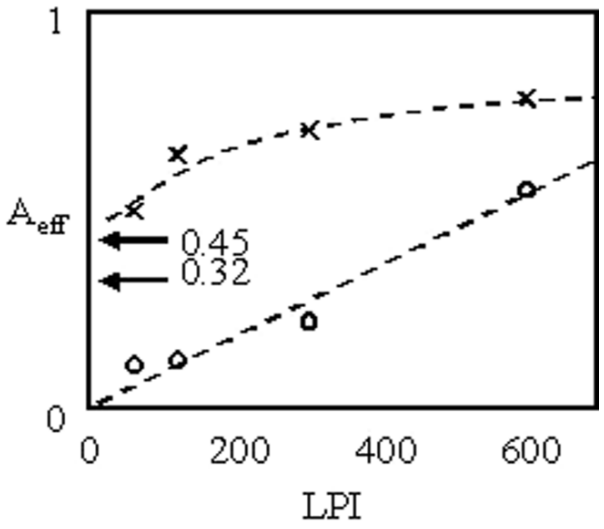

Figure 9. Efficiency factors, A_{eff}, versus lines per inch, lpi, for cyan toner and black toner.

cyan (S = 0) and the black (S > 0) represent two different kinds of behavior, but both groups show an increase in A_{eff} as lpi increases, in agreement with expectation.

In the limit as lpi approaches infinity, the printed images are assumed to behave as perfect continuous tone systems at all values of C. Thus in the limit lpi → ∞, $A_{eff} = 1$. Figure 9 suggests this limit is reached only for very high frequency halftones (lpi ≥ 1200 lpi). Of much more interest is the limit as lpi → 0. In this limit the halftones should behave as ideal Murray–Davies halftones, Eq. (1). In this limit, we substitute the Murray–Davies equation for R into Eq. (10) to find the limiting behavior of f(C), shown in Eq. (11). This should represent the lowest ink efficiency (maximum ink anti-gain) one would observe for a halftone image with non-scattering ink. This equation can be integrated for both the 300 dpi and the 600 dpi systems to find limiting values of A_{eff}. The result depends somewhat on the functional relationship between C and F_n, so the results are $A_{eff} = 0.45$ for the 300 dpi printer and $A_{eff} = 0.32$ for the 600 dpi printer. These limiting values are shown in Fig. 8, and it is evident the data for the cyan toner (S = 0) is approaching the generally expected limit, within experimental uncertainty.

$$f(C) = \frac{log\left[R_g\right] - \mathrm{Log}\left[F_n \cdot R_k + (1 - F_n)R_g\right]}{\varepsilon_o \cdot C} \tag{11}$$

The limiting behavior for lpi → 0 for the black toner (S > 0) requires investigation of the Kubelka–Munk Eq. (6). We write the expression for the absorption coefficient, K, using the absorption efficiency function, f(C), as shown in Eq. (12).

$$K(C) = 2.303 \cdot \varepsilon_o \cdot f(C) \cdot \frac{C}{L} \tag{12}$$

In the low frequency limit of lpi → 0, the halftone behaves as an ideal Murray–Davies halftone. This is true for the toner with S > 0 as well as S = 0. Conceptually we could substitute the Murray–Davies equation for R and Eq. (12) for K into the Kubelka–Munk Eq. (6) and solve for the absorption efficiency f(C). However, it is difficult to invert the Kubelka–Munk equation analytically, so it is difficult to estimate a limit for f as C → 0. Nevertheless, some insights can be gleaned by replacing C in Eq. (12) by the assumed scattering function $S(C) = C \cdot S_{max}$ and solving for the efficiency function, Eq. (13).

$$f(C) = \left[\frac{K(C)}{S(C)}\right] \cdot \left[\frac{L \cdot S_{max}}{2.303 \cdot \varepsilon_o}\right] \tag{13}$$

The value of the ratio on the right hand side of Eq. (13) for black toner is approximately 0.1 based on values in Table I. The value of the ration K/S is difficult to extimate as a function of C. However, both have been modeled as linear functions of C. If this is approximately so, then the ratio K/S is expected to be approximately independent of C. At C = 1, the ration K_{max}/S_{max} is a small number < 0.1. Thus, the expectation is that f < 0.1 at C → 0. This is consistent with the data in Table I, displayed as shown in Fig. 8.

Conclusions

For halftone images printed in the typical range 100 < lpi < 600, a continuous tone model appears to be as reasonable as a bilevel mode for describing tone reproduction. Both require significant modifications in order to fit experimental data. Much research has shown that modifications required for a bilevel model are mechanistically associated with spatial effects typically called dot gain. In this report, modifications required for a continuous tone model also appear to be mechanistically associated with spatial effects. To highlight the analogy with dot gain, we have called these effects "ink anti-gain." This report has shown the potential capability of the continuous tone approach and has suggested only a preliminary link to mechanistic effects. Nevertheless, the con-tone approach appears capable of rationalizing tone reproduction in halftone images, and it is suggested that further consideration of this approach both for empirical printer calibration and for mechanistic insights might be of value.

Acknowledgment. The authors express their appreciation to Hewlett-Packard Corporation for their support of this project. Special thanks to Bob Chin, Manager of Digital Technologies in OMNOVA Solutions, Inc., for sponsorship of summer research support for undergraduate student participation in the project.

References

1. J. P. Allebach, Ed., Selected Papers on Digital Halftoning, SPIE Milestone Series, vol. MS154, SPIE Optical Eng. Press, Bellingham, WA, 1999.
2. P.G. Engeldrum, The Color Between the Dots, J. Imaging Sci. Technol. **38**, 545 (1994).
3. J. S. Arney, P. G. Engeldrum and H. Zeng, J. Imaging Sci. Technol. **39**, 502 (1995).
4. J.A.C. Yule and W. J. Neilsen, Proc.TAGA, 65 (1951).
5. J.A.C. Yule, D. J. Howe and J. H. Altman, TAPPI, 337 (1967).
6. G. Wyszecki and W.S. Stiles, Color Science: Concepts and Methods, 2nd ed., John Wiley and Sons, NY, 1982, p. 221.